Deformation mechanisms during plane strain compression of 17%Mn steel

Pereloma, E.[1], Pramanik, S.[1], Saleh, A.[1] and Gazder, A.[1]

[1] University of Wollongong, Australia

Advanced high strength steels containing 15-20% of Mn exhibit an attractive combination of mechanical properties due to the deformation accommodation mechanisms of slip, twinning and phase transformation of metastable austenite (face-centred cubic, fcc). Their operation depends on the stacking fault energy of austenite, which in turn is defined by the steel composition. The final microstructure depends on the total strain imposed on the material during deformation as well as the deformation mode. In general, perfect and partial slip occur in metastable austenite. Phase transformation follows two pathways: the formation of body-centred cubic (bcc) martensite directly from austenite or via prior austenite transformation to hexagonal closed packed (hcp) martensite. Phases formed at lower strains are also subjected to deformation at higher strains. There has been disagreement as to whether and/or how epsilon martensite accommodates deformation. In this research, we addressed this issue by applying high resolution scanning transmission electron microscopy (STEM) and electron back-scattering diffraction (EBSD).

A hot rolled 17% Mn steel was subjected to room temperature plane strain compression up to 20% thickness reduction. In addition, cold rolling to 42, 66 and 88% reduction was performed. The evolution of microstructure with strain was tracked by TEM (Fig. 1) and EBSD. The general trend involved a decrease in austenite fraction and an initial increase in hcp martensite fraction up to 20% thickness reduction followed by the predominance of bcc martensite formation at higher thickness reductions. The STEM observations showed that intrinsic stacking faults (ISF) in austenite served as the nucleation sites for hcp martensite. The as-quenched and deformation-induced nano-sized (<20 nm thickness) hcp martensite do not contain ISFs. With increase of strain to 10% thickness reduction, the development of I_2-type ISFs was observed in hcp martensite (> 20 nm thickness). At 20% thickness reduction, I_2 -type ISFs transition to I_1 -type ISFs (Fig. 2). At the same time, the formation of $\{10\bar{1}2\}\langle\bar{1}011\rangle$ extension twins was also observed. Thus, for the first time, direct evidence of deformation accommodation by hcp martensite was obtained and its mechanism proposed. Concurrently, bcc martensite formation takes place at the intersections of or within hcp martensite laths. With higher thickness reduction, hcp martensite transforms to bcc martensite. The remnant hcp martensite at 66-88% reduction is present in thin, elongated morphologies between bcc crystals. The latter phase deforms by slip and exhibits the formation of local macroscopic shear bands.

This work was supported by the Australian Research Council-Discovery Project (DP130101882).

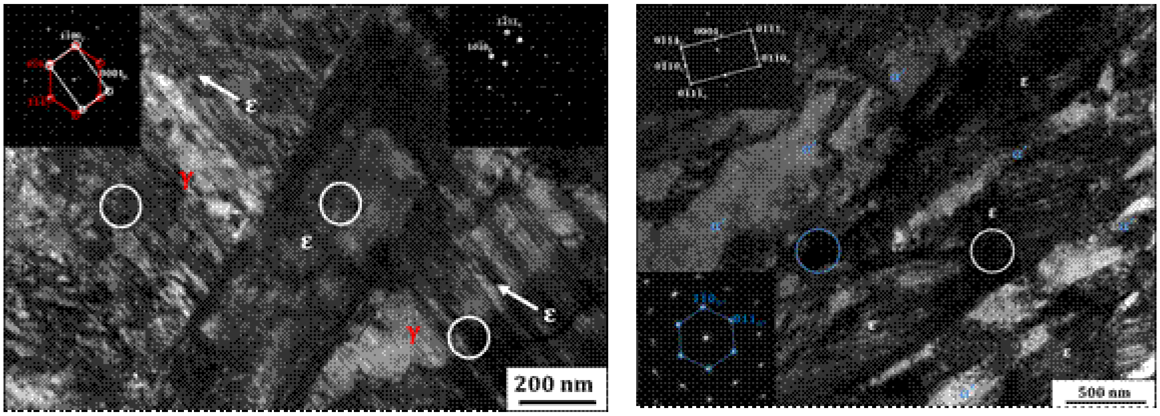

(a) (b)

Fig. 1 TEM micrographs showing microstructure after plane strain compression/cold-rolling to (a) 20% and (b) 42% thickness reduction. The inset diffraction patterns in Figs. 1a, 1b are from the blue or white circular regions. In Fig. 1a the zone axes of the diffraction patterns in the top left are $[11\bar{2}0]_{\varepsilon}$, $[101]_{\gamma}$and top right is $[\bar{1}2\bar{1}6]_{\varepsilon}$. In Fig. 1b the zone axes of the diffraction patterns in the top right and bottom right are $[2\bar{1}\bar{1}0]_{\varepsilon}$and $[\bar{1}\bar{1}1]_{\alpha'}$. The top left diffraction pattern (Fig. 1a) indicate Shoji-Nishiyama orientation relationship.

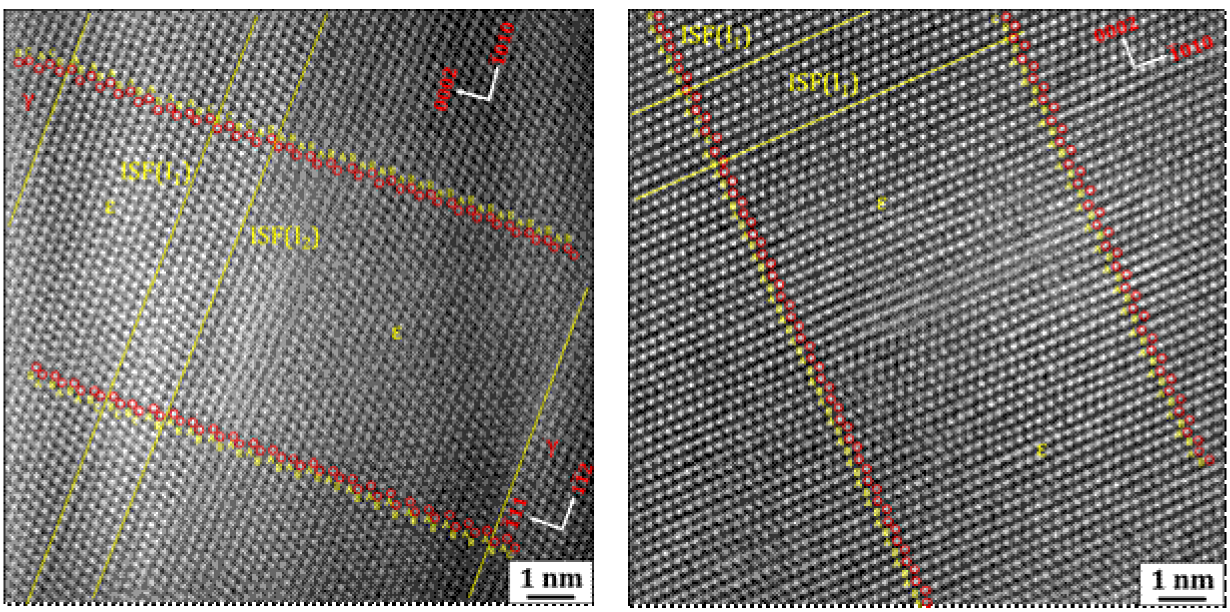

(a) (b)

Fig. 2 HAADF STEM micrographs showing ε-ISFs of type I_2 and I_1 after plane strain compression/cold-rolling to (a) 15% and (b) 42% thickness reduction. Zone axes are $[110]_{\gamma}$, $[\bar{1}2\bar{1}0]_{\varepsilon}$in Fig. 2a and $[\bar{1}2\bar{1}0]_{\varepsilon}$in Fig. 2b.